Micro-Gal laser absolute gravimeter based on high precision heterodyne interferometer

Zhiping Zhang (张志平), Zhaogu Cheng (程兆谷), Zhaoyu Qin (覃兆宇), and Jianqiang Zhu (朱健强)

Shanghai Institute of Optics and Fine Mechanics, Chinese Academy of Sciences, Shanghai 201800

Received December 5, 2006

A micro-Gal absolute gravimeter based on high-precision and high-stability heterodyne interferometer is presented. The distance measuring technology of the gravimeter is studied in detail. The experimental results of distance measuring for a free-falling motion show that the high-precision heterodyne interferometer described in this paper can meet the demand of a micro-Gal absolute gravimeter with relative uncertainty of 6.4×10^{-9}. Moreover, the heterodyne interferometer is more stable than the Mach-Zehnder interferometer (MZI) which is widely used in present absolute gravimeters.

OCIS codes: 120.0120, 120.3940, 120.3180.

The gravity g is a physical quantity varying in time and space. The value of g depends, mainly, on the latitude, the mass distribution in the Earth's interior, the Earth's rotation (velocity and position of the rotation axis), and the relative positions of the Moon and the Sun which cause the tides. The common gravity unit used in field measurements of gravity is the Gal (1 Gal = 1 cm/s^2). The determination of g is very important in many areas such as geophysics, geology, geodesy, and metrology[1,2]. Gravity data is also used for petroleum and mineral exploration as well as geoid and tidal parameter definition[3]. In recent years, the measuring and development of absolute gravity still attract much attention because of exigent requirements in the above-mentioned application areas[4−7]. The most popular absolute gravimeter is FG5 made in USA[1], with the precision of several micro-Gals.

In present laser absolute gravimeters (for example FG5), a rubidium atomic time base provides the time scale for the accurate timing and a Mach-Zehnder interferometer (MZI) provides the length scale for the accurate positioning[1,2]. Compared with the measurement of time, more problem is the measurement of distance[8].

In this paper, a micro-Gal laser absolute gravimeter based on a heterodyne interferometer with higher precision and higher stability (not MZI) is presented. And an interference fringe occurs in each $\lambda/512$ of the laser beam, which can further enhance the positioning precision than the MZI.

The relationship between distance and time during free-falling motion is shown in Fig. 1. According to the free-falling law, the gravity g can be given as

$$g = \frac{2\left(\frac{S_2}{T_2} - \frac{S_1}{T_1}\right)}{T_2 - T_1}, \quad (1)$$

where $S_1 = x_2 - x_1$ and $S_2 = x_3 - x_1$, which are measured by a heterodyne interferometer; $T_1 = t_2 - t_1$ and $T_2 = t_3 - t_1$, which are measured by a time interval measurement. x_1, x_2, and x_3 are the coordinates of displacements, and t_1, t_2, t_3 are the coordinates of time, and they are all shown in Fig. 1.

A total of several hundreds time-position points are recorded over the course of each drop. Then the time-position data are performed by a least square fit according to[1,4]

$$x(t)_i = x_0 + v_0\tau_i + \frac{g_0}{2}\left(\tau_i^2 + \frac{1}{12}\gamma\tau_i^4\right), \quad (2)$$

$$\tau_i = t_i - \frac{(x_i - x_0)}{c}, \quad (3)$$

where x_0, v_0, and g_0 are the initial position, velocity, and acceleration at $t = 0$, c is the speed of light, τ_i is the time considering the propagation time of light between the distance of $(x_i - x_0)$, and γ is the vertical gravity gradient which is measured using a relative spring gravimeter and usually equals about 3 μGal/cm. The gravity g is obtained after applying correction data for each drop.

The schematic illustration of the absolute gravimeter is shown in Fig. 2. The drive mechanism is used to lift, drop, and catch the drag-free cart which houses the test mass. The measurement corner-cube is attached to the test mass. Firstly the drag-free cart is lifted to the top of the drive mechanism driven by a direct current (DC) servo motor. Secondly the cart is dropped. At the beginning of a drop, the cart accelerates downwards with an acceleration greater than g. Once a certain separation between the cart and the test mass is reached, the cart slows down and tracks the test mass, maintaining a constant separation of a few millimeters. By keeping track of the cart position using a shaft encoder, and using the interferometer to establish the test mass position, the

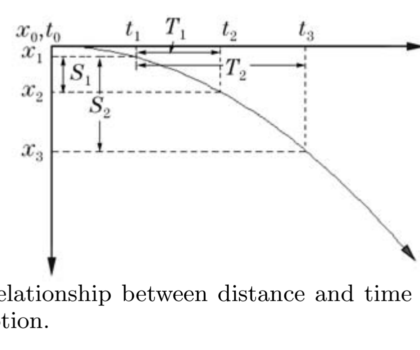

Fig. 1. Relationship between distance and time during free-falling motion.

1671-7694/2007/060344-03

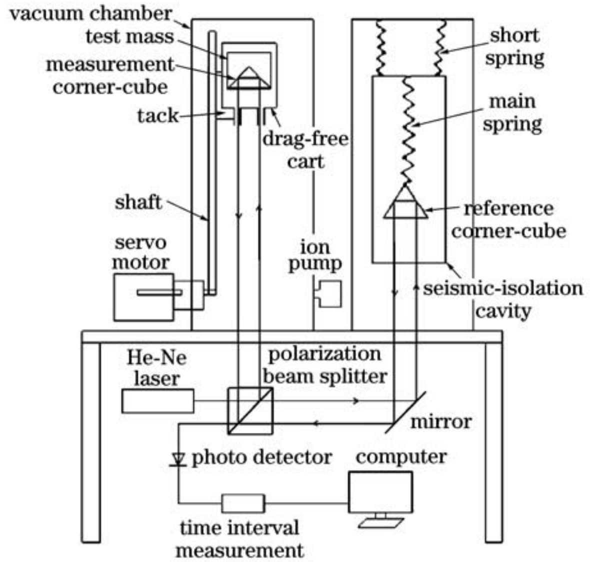

Fig. 2. Schematic illustration of the absolute gravimeter.

distance between the cart and the mass can be determined by using the servo-motor drive system to control the position and velocity of the cart. During the free falling of the test mass, the distance of corner-cube is measured by a high-precision heterodyne interferometer and the time which takes to fall some predetermined distance is measured by a time interval measurement. Finally, at the bottom of the drop, the cart gently catches the test mass. And the measuring course abovementioned is repeated. Then these time-position pairs are fitted by a suitable motion model in a least-square algorithm and the gravity value is obtained.

Though the vacuum chamber is evacuated by an ion pump, there are still some residual air molecules. The drag-free cart effectively pushes these molecules out of the way of the test mass, which is falling behind the cart. In addition to reducing drag, the cart also reduces magnetic and electrostatic forces on the test mass. The reference corner-cube of interferometer is hung by a superspring system to keep from experiencing high-frequency vertical ground shaking. This ensures that any change in the length of the test beam is due only to the acceleration of the dropped object. The corner-cubes are three-surface mirrors which have the special optical property that the reflected beam is always parallel to the incident beam. Moreover, the center of the test mass and the optical center of the measurement corner-cube must be co-located to the greatest extent in order to eliminate the rotation error.

The uncertainty of g is the synthesization of the uncertainties of time and distance. The relative uncertainty can be given by

$$\frac{\Delta g}{g} = \sqrt{(\frac{1}{S})^2 U_{\mathrm{S}}^2 + (\frac{2}{T})^2 U_{\mathrm{T}}^2}, \tag{4}$$

where U_{S} and U_{T} are the uncertainties of distance and time, respectively.

An interference fringe occurs each $\lambda/512$ of the laser beam crossed by the free-falling test mass in our heterodyne interferometer. The interference signal is recorded by a detector and sent to a zero-crossing discriminator (ZCD) after removing the DC component. The ZCD produces a transistor-transistor logic (TTL) pulse each time, the input voltage crosses the zero level in the positive going direction. The TTL pulses are scaled by a pre-defined factor, and the times of occurrence of scaled pulses are measured as to a starting reference time by a time interval measurement (synchronized with a rubidium clock). The sketch of time interval measuring is shown in Fig. 3. The time interval T measured can be shown as

$$T = nT_{\mathrm{p}} + \Delta T_1 - \Delta T_2, \tag{5}$$

where n is a positive integrer, T_{p} is the pulse duration of clock, ΔT_1 and ΔT_2 are the fraction components which are measured by interpolating method. The time interval measurement based on interpolating method or tapped delay line method has the uncertainty of the order of 10^{-11} s[9], which is precise enough for micro-Gal gravimeter. So the uncertainty of gravimeter is mainly determined by the laser interferometer.

The detail of distance measuring interferometer is shown in Fig. 4. It is a heterodyne interferometer, which has higher precision and stability than MZIs used in present gravimeters such as FG5. Moreover, the heterodyne interferometer has advantages of anti-jamming and large measuring range[10−12]. In Fig. 4, the measurement corner-cube is attached to the test mass (free-falling body), and the reference corner-cube is fixed. And the interference fringe signal is shown in Fig. 5. The increase in the fringe signal frequency as the test body (also measurement corner-cube) free falls is obvious in the figure.

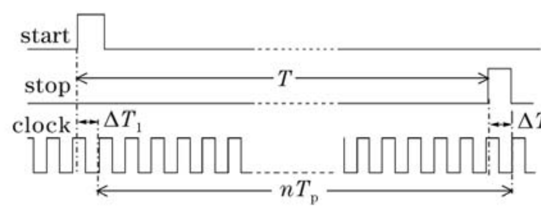

Fig. 3. Sketch of time interval measuring.

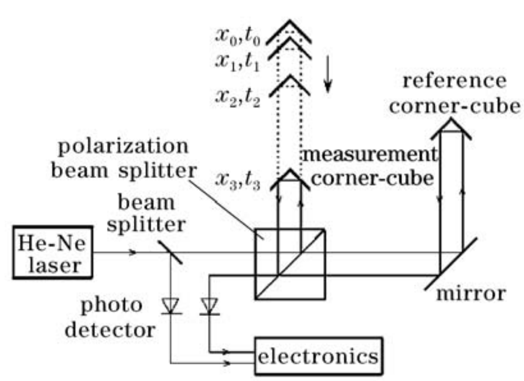

Fig. 4. Displacement measuring of free-falling body.

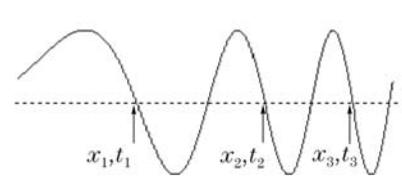

Fig. 5. Optical fringe signal during the free-falling process.

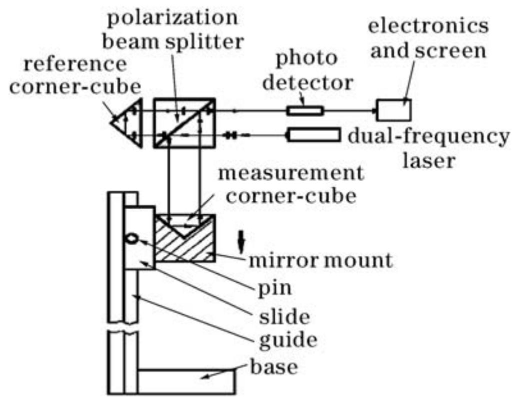

Fig. 6. Experimental setup for measuring the free-falling body.

In the case of measuring the distance of the free-falling body, the most doubt is the influence of the acceleration on precision. The literatures about the influence are still little. An experimental setup was established to observe the measuring precision during the free-falling motion, as shown in Fig. 6. In order to simplify the setup, we did not build the vacuum chamber system, the whole operation was under ordinary laboratory conditions. The guide is precisely machined and lubricated, and sternly upright to the horizontal line. Without considering the air resistance and friction, the course that measurement corner-cube moves along the guide can be taken as free-falling motion.

The laser head used in the experiment is a He-Ne laser with automatically tuned Zeeman-split two-frequency output. Its vacuum wavelength is 632.991354 nm, typical short term (1 hour) wavelength stability is ±0.002 ppm, and calibrated wavelength accuracy is ±0.02 ppm. A subdivision factor of 1/512 was obtained with the interferometer system shown in Fig. 6, so an improved resolution of $\lambda/512$ (i.e., 1.24 nm) can be achieved. Forty time-position pairs were recorded in a single dropping with the distance of 0.1 m. The measurement results are shown in Fig. 7.

According to the data, we can calculate the uncertainty of distance. The uncertainty of distance measurement can be given by[13]

$$U_{\mathrm{S}} = \frac{S_x}{\sqrt{n}}, \tag{6}$$

where n is the measured times, and S_x is the standard deviation. From the data in Fig. 7, we can calculate that

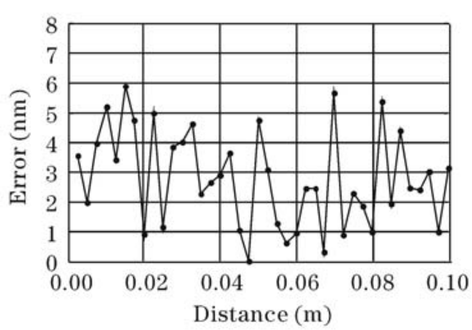

Fig. 7. Measurement errors during the free-falling motion.

$S_x = 4.03$ nm. So the uncertainty of distance U_{S} is 0.64 nm, i.e., 6.4×10^{-10} m. The dropping time corresponding to the distance of 0.1 m is 0.14 s. So according to Eq. (4), the relative uncertainty of absolute gravity $\frac{\Delta g}{g}$ is about 6.4×10^{-9}, which corresponds to the precision of 6.4 micro-Gals.

If the experiment is operated under the condition of vacuum, the reference corner-cube is hung by a super-spring system and the time-position data are sampled for several hundred times during each dropping, the relative uncertainty of gravity can be further lower and reach the order of 10^{-10}.

In conclusion, the gravity g is determined jointly by the distance and time of a free-falling body. The time interval measurement based on rubidium clock has uncertainty of the order of 10^{-11} s, which is enough for micro-Gal gravimeter, so the distance measuring technology of the gravimeter based on heterodyne interferometer is emphasized. An experimental setup for studying the measuring precision of distance during the free-falling motion has been established. The experimental results show that the high-precision heterodyne interferometer described in this paper can meet the demand of a micro-Gal laser absolute gravimeter, and the heterodyne interferometer is more stable than the MZI which is widely used in present absolute gravimeters.

Z. Zhang's e-mail address is zzp8101@siom.ac.cn.

References

1. M. Van Camp, T. Camelbeeck, and P. Richard, Physical Magazine, Journal of the Belgian Society **25,** 161 (2003).
2. W. E. Carter, G. Peter, G. S. Sasagawa, F. J. Klopping, K. A. Berstis, R. L. Hilt, P. Nelson, G. L. Christy, T. M. Niebauer, W. Hollander, H. Seeger, B. Richter, H. Wilmes, and A. Lothammer, EOS Trans. Am. Geophys. Union **75,** 90 (1994).
3. J. M. Brown, T. M. Niebauer, B. Richter, F. J. Klopping, J. G. Valentine, and W. K. Buxton, "Miniaturized gravimeter may greatly improve measurements" EOS Online Supplement, http://www.agu.org/eos_elec/99144e.html.
4. E. R. Pujol, Física de la Tierra. **17,** 147 (2005).
5. G. D'Agostino, S. Desogus, A. Germak, C. Origlia, and G. Barbato, Journées Luxembourgeoises de Géodynamique, Nov. 8 (2004).
6. A. L. Vitouchkine and J. E. Faller, Metrologia **41,** L19 (2004).
7. P. Baldi, E. G. Campari, G. Casula, S. Focardi, G. Levi, and F. Palmonari, Phys. Rev. D **71,** 022002 (2005).
8. G. P. Arnautov, L. D. Gik, E. N. Kalish, V. P. Koronkevitch, I. S. Malyshev, Yu. E. Nesterikhin, Yu. F. Stus, and G. G. Tarasov, Appl. Opt. **13,** 310 (1974).
9. Y. Zhang and P. Huang, Progress in Astronomy (in Chinese) **24,** 1 (2006).
10. H. Gao, Z. Cheng, Z. Ning, P. Cui, and H. Huang, Chin. Opt. Lett. **3,** 513 (2005).
11. F. C. Demarest, Meas. Sci. Technol. **9,** 1024 (1998).
12. Z. Cheng, H. Gao, Z. Zhang, H. Huang, and J. Zhu, Appl. Opt. **45,** 2246 (2006).
13. W. Chen, "Least Uncertainty Estimation Theory and Its Applications" (in Chinese) Master Thesis (Wuhan University, 2005) pp.9—10.